Mechanisms of Cell Shape Change: The Cytomechanics of Cellular Response to Chemical Environment and Mechanical Loading

Dany Spencer Adams

Department of Zoology (NJ-15), University of Washington, Seattle, Washington 98195

Abstract. Processes such as cell locomotion and morphogenesis depend on both the generation of force by cytoskeletal elements and the response of the cell to the resulting mechanical loads. Many widely accepted theoretical models of processes involving cell shape change are based on untested hypotheses about the interaction of these two components of cell shape change. I have quantified the mechanical responses of cytoplasm to various chemical environments and mechanical loading regimes to understand better the mechanisms of cell shape change and to address the validity of these models. Measurements of cell mechanical properties were made with strands of cytoplasm submerged in media containing detergent to permeabilize the plasma membrane, thus allowing control over intracellular milieu. Experiments were performed with equipment that generated sinusoidally varying length changes of isolated strands of cytoplasm from *Physarum polycephalum*. Results indicate that stiffness, elasticity, and viscosity of cytoplasm all increase with increasing concentration of Ca^{2+}, Mg^{2+}, and ATP, and decrease with increasing magnitude and rate of deformation. These results specifically challenge assumptions underlying mathematical models of morphogenetic events such as epithelial folding and cell division, and further suggest that gelation may depend on both actin cross-linking and actin polymerization.

FUNDAMENTAL to understanding both morphogenesis and cell locomotion is an understanding of the mechanisms of cell shape changes. Current ideas about those mechanisms are based largely on two types of approaches: (a) mathematical modeling (e.g., Odell et al., 1981; Mittenthal and Mazo, 1983; Oster et al., 1983; White and Borisy, 1983; Oster and Odell, 1984; Belintsev et al., 1987); and (b) experimental characterization of the distribution and activity of microfilament- and microtubule-based force generating systems (e.g., Byers and Porter, 1964; Pollard and Ito, 1970; Spooner and Wessells, 1972; Burnside, 1973; Stopak and Harris, 1982; Priess and Hirsh, 1986). Less frequently examined, although equally critical, are the responses of the cell to the mechanical loads imposed on them by their cytoskeletons or by external forces (Waddington, 1942; Odell et al., 1981; Condeelis, 1983; Elson, 1988). Those responses are prescribed by mechanical properties of the cell such as stiffness, elasticity, and viscosity.

Although many researchers have contributed to the task of characterizing the mechanical properties of cytoplasm (e.g., Seifriz, 1952; Hiramoto, 1970, 1976; Yoshimoto and Kamiya, 1978; Achenbach and Wohlfarth-Bottermann, 1980; Matsumura et al., 1980; Sato et al., 1983) no one has yet produced a comprehensive description that considers both the nature of the loads and their time history (Elson, 1988). As a result, mathematical models of morphogenesis have relied largely on postulated mechanical properties rather than empirically derived values (e.g., Oster and Odell, 1984).

Likewise, we still lack a complete understanding of how cell mechanical properties are regulated (e.g., Ueda et al., 1978; Hasegawa et al., 1980; Ogihara and Tonomura, 1982; Ogihara, 1982). Cells could potentially exploit both mechanical and chemical information in modulating their properties and thus their behavior; changes in intracellular ionic concentrations are well documented (e.g., Taylor et al., 1973; Yoshimoto et al., 1981a,b; Miller, 1988), and during cell shape change cytoplasm experiences a range of forces (Waddington, 1942; Rappaport, 1967; Stopak and Harris, 1982). Therefore, to produce a comprehensive description of cytoplasmic mechanical properties and their regulation, the effects of both applied forces and chemistry must be characterized.

Furthermore, to produce the kind of characterization that is needed, the following known properties of cytoplasm should be considered a priori: (a) Cytoplasm is viscoelastic. The mechanical properties of cytoplasm depend on both the magnitude and the rate of the applied forces (Seifriz, 1952; Ferry, 1980; Sato et al., 1983, 1987); and (b) cell properties can vary with the concentrations of different intracellular ions (Ueda et al., 1978; Yoshimoto et al., 1981a,b; Pollard and Mooseker, 1981) as well as the concentration of ATP (Matsumura et al., 1980; Ogihara, 1982).

Characterization of cytoplasm mechanical properties can also yield information about the ultrastructure of cytoplasm. By exploring how a material (in this case cytoplasm) reacts to forces such as tension (pulling) or compression (pushing) it is possible to deduce information about the organization of that material (Elson, 1988). There is both theoretical and empirical evidence behind the assertion that the magnitude and time course of a material's response to tensile or compressive loads is determined by, and thus indicative of, the underlying structure of that material. Thus, measurements of the response of cytoplasm to mechanical loads can provide a window on the structure of cytoplasm.

The work described herein quantifies the mechanical properties of cytoplasm and explores how those properties vary with changes in the mechanical and chemical environment. From these descriptions it is possible to (a) address the validity of some important models of morphogenesis, (b) draw inferences about the changing structure of cytoplasm and how those changes may be regulated, and (c) make hypotheses about how cell mechanical properties might constrain or be exploited by the cell during the shape changes that underlie locomotion and morphogenesis.

A useful system for studies of cellular mechanics has been cytoplasm from the large plasmodia of the acellular slime mold *Physarum polycephalum* (Kamiya, 1959). Actomyosin in the tubelike ectoplasm of these cells produces a radial contraction of the tube that causes shuttle streaming, a rapid bidirectional translocation of the central, fluid endoplasm (Kamiya, 1981). The large tubelike strands are easily excised and manipulated without loss of their ability to generate force, making them convenient for experimental manipulation (Kamiya, 1959). Because it is an actomyosin system, it is believed that the force production by these strands depends on the concentration of calcium ions, magnesium ions, and ATP—hereinafter [Ca^{2+}], [Mg^{2+}], and [ATP], (Yoshimoto et al., 1981a,b; Pollard and Mooseker, 1981). Furthermore, there is evidence that the magnitude and rate of the applied forces do indeed affect the mechanical behavior of *Physarum* cytoplasm (Yoshimoto and Kamiya, 1978; Sato et al., 1987). Thus, strands of *Physarum* are an appropriate and convenient system for this study of cytoplasmic mechanical properties.

To quantify these properties, I exploited an approach that uses sinusoidal length changes to determine the dynamic response of cytoplasm to mechanical loads (Tidball and Daniel, 1986; Meyhöfer and Daniel, 1990). I combined this dynamic mechanical testing with the use of mild detergent treatments that allowed control over the intracellular ionic environment. The results describe how the stiffness, elasticity, and viscosity of *Physarum* cytoplasm varied with changes in both the chemical and mechanical environment. These data indicate that cellular mechanical properties depend significantly upon both the rate and the magnitude of deformation as well as intracellular levels of calcium, magnesium, and ATP. Furthermore, these results are consistent with the hypothesis that stiffening of the cytoplasm is the result of both actin–myosin crosslinking and actin polymerization.

Materials and Methods

Maintenance of Physarum and Generation of Strands

Physarum polycephalum plasmodia (Carolina Biological Supply Co., Bur-

lington, NC) were fed organic rolled oats and housed on damp filter paper set in glass petri dishes (after the methods of Camp, 1936). The dishes were kept in a dark aquarium and floated on water to maintain high humidity. New, small cultures were fed frequently to encourage rapid growth without branching. When the cultures covered approximately half of the dish, rations were reduced sharply to stimulate the appearance of thick strands of cytoplasm that connected the central portion of the organism to the many small branches at the distal tip. New cultures were easily started by collecting branches from the water surface and placing them on new filter paper. Thus collected, new cultures were ready to be fed in ~6 h. Individual cultures grew and produced strands reliably for ~2 wk.

Isolation of Cytoplasmic Strands

Single strands, ~0.5 mm and uniform in diameter, and between 5- and 10-mm long, that were mostly free of the thick glycocalyx that usually surrounds strands, were excised with forceps from the vertical sides of the dishes and transferred to the apparatus on a drop of water to prevent desiccation. Each end of the strand was attached with cyanoacrylate to a holder. These holders formed part of a mechanical measurement device (see below) and were constructed by denting one end of a small length of polyethylene tubing to create a trough for holding the strand. The open end of the tube was slipped over a blunt needle that was permanently attached to the apparatus. After 1-2 min submerged in water, the attached strand was submerged for 3-5 min in a 0.01% (wt/vol) saponin solution (see Table I) to permeabilize the plasma membrane (Stout and Diecke, 1983; Murakami, 1987) thus permitting control of intracellular levels of Ca^{2+}, Mg^{2+}, and ATP. The strand was then transferred through media of intermediate [Ca^{2+}] to the testing medium (Table I); all media contained 0.005% (wt/vol) saponin to insure continued permeability of the membrane. The holders were then moved apart until the strand was under a tension detectable on an oscilloscope. The protoplasmic strand was subject to strains no greater than 25% of the initial unloaded length. After 1-2 min, the diameter and length of the strand were measured to the nearest 0.05 mm with an ocular micrometer mounted in a dissecting microscope. After that measurement, the strand was resubmerged and allowed to sit undisturbed for at least 3 min before testing.

Apparatus

A device modified from the methods of Meyhöfer and Daniel (1990) was designed to deliver sinusoidal deformations to cytoplasmic strands while simultaneously recording instantaneous force on the strand. The strand was suspended by holders (see above) between a piezoelectric crystal and the force platform. Deflection of such a crystal is proportional to the applied voltage which, in this apparatus, was controlled by computer. Analog sine waves sent to the crystal generated sinusoidally varying deformations of the attached *Physarum* strand. The resulting tensile force in the strand was monitored at the opposite end by a force transducer. The transducer consisted of two semiconductor strain gauges (Entran Devices Inc., Fairfield, NJ), one mounted on each side of a 8 × 7 mm piece of stainless steel. The transducer had a sensitivity of 1.2×10^{-4} N/V and a compliance of 6.5×10^{-6} m/V. Each gauge formed one arm of a Wheatstone bridge excited at 4.0 V whose output was amplified with standard op-amp circuitry. The voltage output of the amplifier was calibrated for deflection of the platform by deforming the needle a known distance. The output was calibrated for force by hanging known weights from the tip of the needle and the deflection of the crystal was assumed to be unaffected by the attached strand, thus, deflection of the crystal was calculated as being directly proportional to the applied voltage. The apparatus was calibrated by hanging known weights from the force platform and the accuracy of the apparatus was confirmed by measuring known properties of viscid spider silk and rubber.

Experimental Protocol

The cytoplasm, and specifically the polymerization state of the actin in the endoplasm of *Physarum*, are known to change significantly with each 1-min half-cycle of shuttle streaming (Wohlfarth-Botterman, 1987); therefore, a given strain and strain rate were applied for at least 1 min before recording values to allow time for any reorganization of the cytoplasm. This brought to a total of 5-6 min that strands were submerged in any given medium before testing began. Each strand was loaded at six different strains, ε, defined as change in length over initial length, $\Delta L/L_o$ (see also below), ranging from 0.013 to 2.9% at a constant rate, or at six different strain rates ($2\pi f \epsilon$ where f is frequency) ranging from 0.002 to 0.059 rad/s with a constant

Table I. Targeted Ionic Concentrations of Media

	$[Ca^{2+}]$	$[K^+]$	$[Na^+]$	[ATP]	$[Mg^+]$	Saponin
						%
Saponin	1.0×10^{-6}	3.8×10^{-2}	4.0×10^{-3}	2.5×10^{-4}	0.0	0.010
ATP No Mg (Figs. 3–5)	1.0×10^{-3}	3.8×10^{-2}	4.0×10^{-3}	5.0×10^{-4}	0.0	0.005
	1.0×10^{-4}	"	"	"	"	"
	1.0×10^{-5}	"	"	"	"	"
	1.0×10^{-6}	"	"	"	"	"
	1.0×10^{-7}	"	"	"	"	"
ATP + Mg (Fig. 6)	1.0×10^{-4}	3.75×10^{-2}	4.0×10^{-3}	5.0×10^{-4}	5.0×10^{-4}	0.005
	1.5×10^{-5}	"	"	"	"	"
	1.0×10^{-7}	"	"	"	"	"
No ATP No Mg (Fig. 7)	1.0×10^{-3}	3.8×10^{-2}	4.0×10^{-3}	0.0	0.0	0.005
	1.0×10^{-5}	"	"	"	"	"
	1.0×10^{-7}	"	"	"	"	"

Targeted ionic concentrations of solutions used in experiments. All solutions contained 4 mM EGTA and 5 mM Hepes. Compositions were determined using software based on Fabiato and Fabiato (1979). All values represent molarities except saponin which is in percent wt/vol.

strain. A medium with a different $[Ca^{2+}]$ was then substituted, and the test was run again. A few strands were also tested in a third medium. Experiments to test for the effect of $[Mg^{2+}]$ and [ATP] were run under conditions of varying strain. Data recorded at the resonant frequency of the apparatus was discarded and the resonant frequency of the cytoplasm was assumed to be close to that of water and thus well outside the range of frequencies examined in these experiments. A given strand was used for no more than 60 min. Preliminary tests showed that after this time there is a precipitous decline in all values measured that appeared to be because of the strand detaching itself from the holder (data not shown). Periodically, a strand was placed on damp filter paper at the end of testing to determine whether testing had caused any serious damage. In all cases, those strands resumed an apparently normal morphology and locomotion.

Data Analysis

For each strain or strain rate that was applied, I recorded voltage data (see above) generated during 10 oscillations of the strand. These data were immediately converted to instantaneous stress and strain values (Fig. 1 a). Stress (σ), the force per cross-sectional area, is determined from the voltage output of the force platform and the measurement of strand diameter (strands were assumed to be circular in cross section). Strain (ϵ), the percent change in length, was determined by calculating the net difference in deflection of the crystal and the force platform (ΔL) and then dividing this difference by the original length of the strand (L_o). Because thermal drift and high frequency noise potentially contaminated the signals, I applied a Fourier transform to the stress and strain curves (Fig. 1 b). Both stress and strain curves were then recreated using only the Fourier coefficients at the driving frequency. The result is a digitally filtered wave representing that portion of the original wave that measures the response of the material to the applied oscillation (Fig. 1 c). This digital filtering is equivalent to an electrical notch filter. Analysis of these reconstructed stress and strain curves yields measurements of the following four mechanical properties (Fig. 2).

The Complex Modulus E*: Stiffness or Total Resistance to Deformation. When you pull on the strand, how hard does it resist stretching? It is calculated by dividing the amplitude of the stress sinusoid by the amplitude of the strain sinusoid ($E^* = \sigma_{max}/\epsilon_{max}$; Fig. 2).

The Elastic or Storage Modulus E': The Elastic Component of the Overall Stiffness. When the material is stretched, how much energy is stored and available for bouncing back? E' is that portion of E* that is in phase with strain and is calculated as follows: $E' = E^* \cos \delta$ (Fig. 2 b).

The Viscous or Loss Modulus E'': The Viscous Component of the

Stiffness. When the material resists stretching, how much energy is lost in permanently deforming the material? E'' is that component of the stiffness that is in phase with the strain rate and is calculated as follows: $E'' = E^* \sin \delta$ (Fig. 2 b). E'' divided by the angular frequency is dynamic viscosity.

The Relative Energy Loss E''/E', or tan δ where δ is the phase angle between the strain and stress curves. (Fig. 2 b). In the ratio of the viscous (energy losing) to the elastic (energy storing) behavior, tan δ is a measure of energy lost in deformation. Higher ratios mean more fluid-like, lower ratios mean more solid-like (Ferry, 1980). A preliminary analysis of these data was originally presented in Adams (1990). A higher signal to noise ratio was required for data to be included in the current analysis. This ratio was determined from visual examination of the Fourier transform of the unfiltered signal (Fig. 1 b). The examinations were done blind with respect to treatment. While the decision to include or exclude data was to some degree subjective, the choice was made a priori to err on the careful side. That is, the only data included were from signals where it was absolutely clear that the amplitude of the signal at the driving frequency far exceeded the amplitude of the noise in the neighborhood of that frequency (compare Figs. 1, b and e). This selection process had the following result: it is virtually certain that the amplitude of the signal used in subsequent calculations of moduli reflected behavior of the sample, not artefacts of thermal or electrical noise in the apparatus. The trade off here is that data from less stiff specimens (those that yield low amplitude signals) were more likely to be swamped by noise and thus disproportionately excluded from the analysis. This may have resulted in overestimates of cytoplasmic stiffness.

Statistical Analysis

The data were analyzed using a form of ANOVA known as linear hypothesis testing (Zar, 1984). A model is devised that predicts the contribution to the variance of each of the variables tested. For example, the following model was fit to the data from Fig. 3 a:

Complex Modulus = overall mean + effect of strain + effect of calcium + effect of individual

This model measures how well variations in strain, calcium, and individual sample explain deviation of the modulus from the overall mean value. The null hypothesis in all cases is that modulus (or tan δ) is not correlated with the variable (i.e., that the slope of the data with respect to the variable is zero). The goodness of fit of the model is then tested. In all cases, $p = 0.05$ is considered significant. Such an analysis provides an initial vantage point from which to explore the relative effects of the treatments in determining
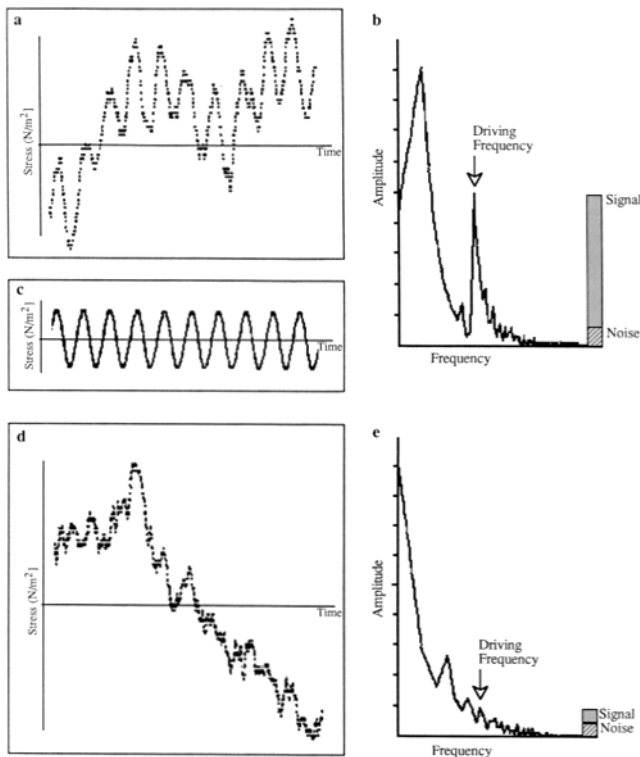
Figure 1. Examples of waves generated in these experiments and illustrations of the digital 'notch filter' using the Fast Fourier transform. (a) Unfiltered stress signal; (b) Fast Fourier transform (FFT) of stress signal shown in a with estimated amplitudes of the signal and noise indicated. Based on the high signal to noise ratio indicated, data from this signal were included in the analysis. (c) Digitally filtered version of signal shown in a. The amplitude of the filtered signal is the sum of amplitudes of the fourier transform at the driving frequency and at two frequencies on either side of the driving frequency. The addition of these extra amplitudes compensates for the likelihood that the driving frequency is not at any one exact FFT frequency. In practice, this correction has little effect on the calculated moduli. (d) Example of unfiltered stress signal. (e) FFT of signal shown in d with estimated amplitude of signal and noise indicated. Based on the low signal to noise ratio indicated, data from this signal were not included in the analysis.

each modulus. Overall trends can be discerned, if not the details of the cytoplasm's behavior.

It is important in this type of analysis to exclude the possibility that a single outlying individual has biased the conclusions. If the effect of any individual sample is significant as determined by the above ANOVA, the data from that offending individual has to be dropped and the hypothesis retested. If there is no change in the conclusion, the data can legitimately be added back to the data set. In the present analysis there was a significant effect of individual on all moduli in all data sets, (tan δ showed no dependence on individual). In a few cases conclusions were affected by the removal of certain individuals. These cases are mentioned in the appropriate figure legends.

Comparisons between data sets, for example between results of experiments done with and without magnesium, are made using the Tukey HSD (Tukey Honestly Significant Difference) or T-method. This is a post hoc comparison of means test (Zar, 1984). All statistical analyses were done using Systat© version 5.0 for the Apple Macintosh.

When the data were examined individually, there was some indication of more complex (i.e., nonlinear) but stereotypical behavior by the cytoplasm. This was true in more than half of the cases. It was not possible to consider the contributions of that behavior using statistical models that assume linearity. Therefore, some specific examples are presented (see Fig. 4).
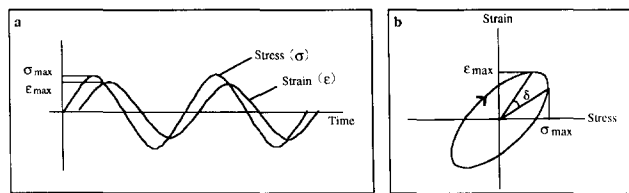

Figure 2. Method for calculating moduli from the signals generated in experiments. (a) Idealized stress, $\sigma(t)$, and strain, $\epsilon(t)$, curves. When sinusoidally varying stresses are imposed on a strand of viscoelastic material the curve representing the resulting strain is shifted in time because of the viscous component of the material. This is in contrast to the elastic component that responds instantaneously to the applied load. (b) Lissajous figure of stress-strain curve indicating the phase angle δ. The oval shape indicates hysteresis or loss of energy during the deformation recovery cycle. If the material were purely elastic, there would be no hysteresis, that is, δ would equal zero and the figure would be an infinitely thin oval, i.e., a line. Such a figure would indicate that the material was purely elastic, that is all of the energy of deformation was stored and available to return the material to its undeformed length upon removal of the load. Rubber is a good example of an elastic material. If the material were purely viscous, there would be no recovery at all, that is, no energy would be available to return the material to its original undeformed length. Water is a good example of a viscous material. See text for further explanation of moduli.

Results

The Effect of the Mechanical Environment

Strain. E*, the overall stiffness, was found to correlate inversely with strain as was the elastic modulus E' (Fig. 3, a and b); thus, as the strand is stretched, it becomes easier to stretch it further. The importance for the cell is that locomotion becomes easier as the magnitude of the movement grows. The data also indicate that E'' (viscous modulus) is significantly correlated with strain (Fig. 3 c) in most, if not all, of the experiments (see legend to Fig. 3 for further explanation). Tan δ (relative energy loss) was not correlated with strain (Fig. 3 d). When the data were examined individually, however, the behavior of more than half of the strands resembled the shapes of the curves shown in Fig. 4. Thus, there may be a significant nonlinearity in the behavior of cytoplasm over the range of conditions examined.

Strain Rate. E* varied inversely with strain rate (Fig. 5 a), suggesting that E' and/or E'' was sensitive to rate. However, neither property showed a statistically significant correlation with rate (Figs. 5 b and 5 c). This is a surprising result in that E* is a function of E' and E''. This result may reflect a small sample size ($n = 47$). The probability values are very close to the alpha level of 0.05 and visual inspection of the E' and tan δ data suggest that E' does decrease with increasing rate. Therefore, it should be noted that these results are equivocal. Tan δ did not vary significantly with rate, however, it did vary with frequency of loading (p = 0.005, data not shown).

The Effect of the Chemical Environment

[Ca²⁺]. E*, the overall stiffness, varied directly with [Ca^{2+}] in all experiments (Figs. 3 a, 5 a, 6 a, and 7 a). E', the elastic modulus, also varied positively with [Ca^{2+}] (Figs. 3 b, 5 b,
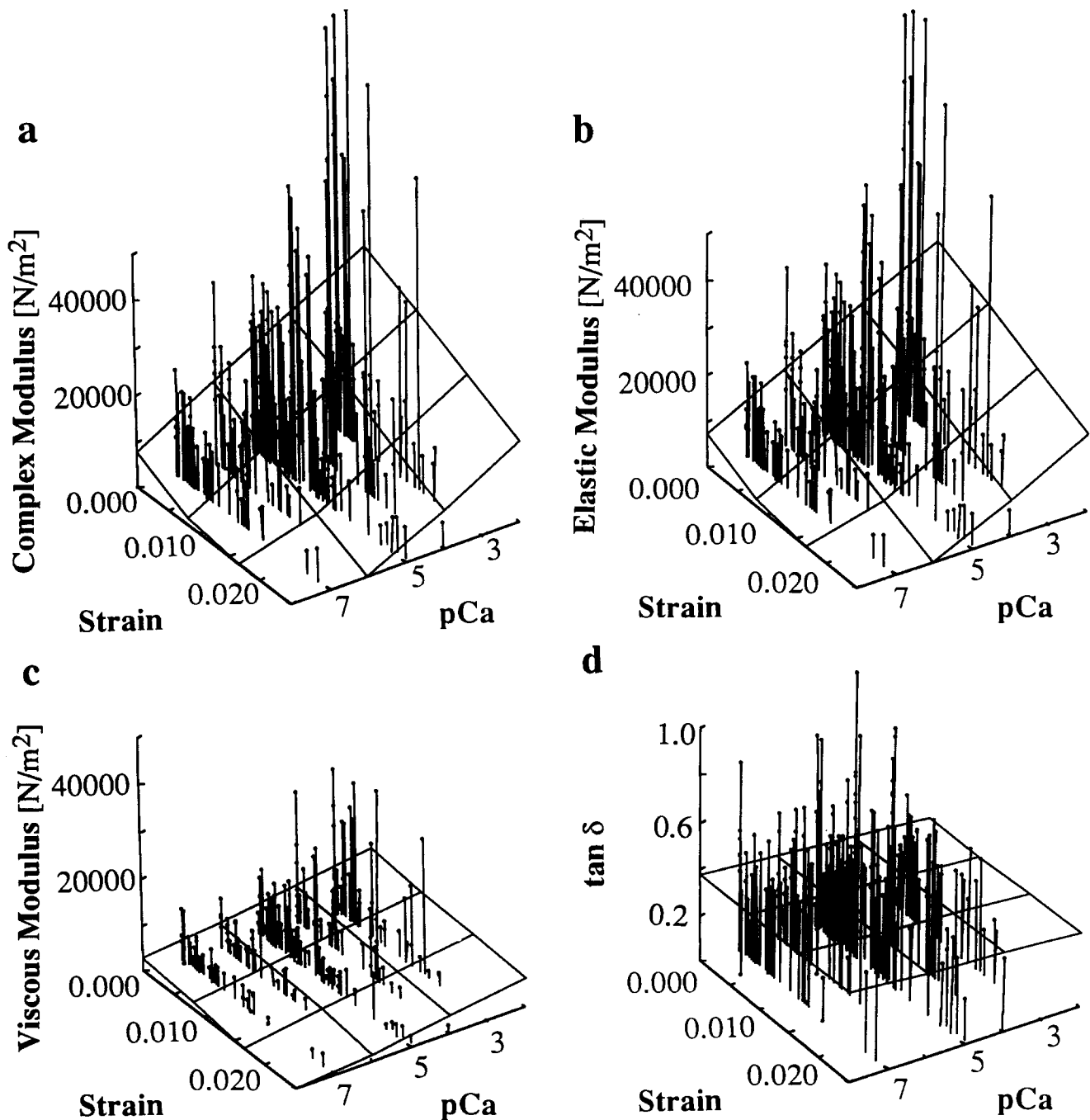
a

Complex Modulus [N/m²]

40000

20000

0.000

0.010

0.020

Strain

7

5

3

pCa

b

Elastic Modulus [N/m²]

40000

20000

0.000

0.010

0.020

Strain

7

5

3

pCa

c

Viscous Modulus [N/m²]

40000

20000

0.000

0.010

0.020

Strain

7

5

3

pCa

d

1.0

0.6

tan δ

0.2

0.000

0.010

0.020

Strain

7

5

3

pCa

Figure 3. Mechanical properties of cytoplasm under conditions of varied strain and $[Ca^{2+}]$ in the absence of Mg^{2+}. For clarity of presentation individual data points are connected by a line to the x-y plane and a plane representing a linear regression through the data has been added. Strain rate was constant at 0.018 ± 0.00035 s^{-1} (mean $\pm$ s.e.); n = 250. (*a*) E*, the complex modulus, showed a significant positive correlation with calcium concentration (p < 0.001) and a significant negative correlation with strain (p < 0.001). (*b*) Like E*, the elastic modulus E' varied directly with calcium concentration (p < 0.001) and indirectly with strain (p < 0.001). (*c*) E ", the viscous modulus, varies directly with calcium concentration (p = 0.055; note that in all other data sets, p < 0.010). Although in this data set E " did not vary significantly with strain (p = 0.229), statistical conclusions from these data were sensitive to the effect of one particular strand. When the data from that one strand was excluded from the analysis, the effect of strain became significant (p = 0.030). In addition, when the three data sets that examined strain effects were combined, the effect of strain on E " was highly significant (p = 0.002). (*d*) The relative energy loss, tan δ, was not correlated with $[Ca^{2+}]$ (p = 0.780) or with strain (p = 0.554).

6 *b*, and 7 *b*). Likewise E", the viscous modulus, increased with increasing $[Ca^{2+}]$ in all experiments (Figs. 3 *c*, 5 *c*, 6 *c*, and 7 *c*; see also figure legends for further explanation). The positive correlation between $[Ca^{2+}]$ and elastic modu-

lus is consistent with the interpretation that the elastic modulus represents mechanical behavior because of the fibrous cytoskeletal network.

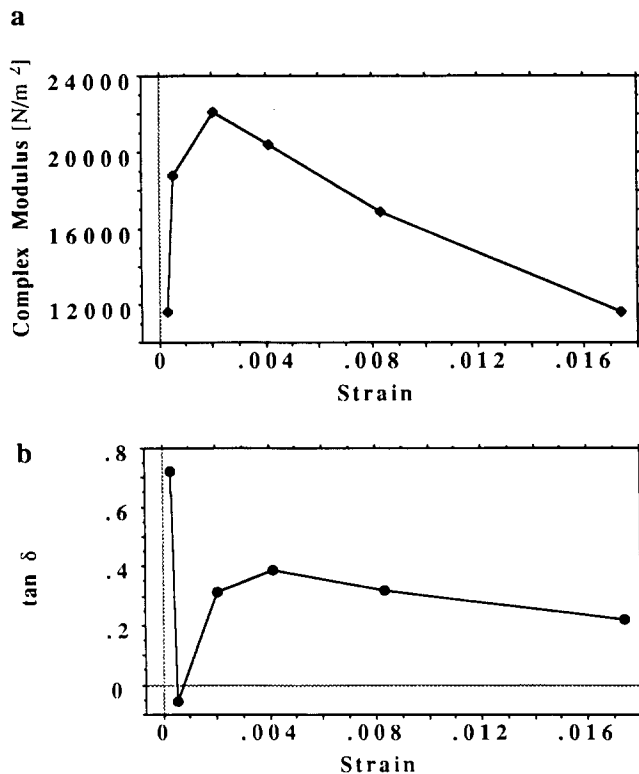*[Mg²⁺].* Overall mean values for E*, E', and E" were all

a

b

Figure 4. Values of properties measured for a single strand of cytoplasm at $[Ca^{2+}] = 10^{-4}$. Strain rate $= 0.018 \pm 0.00035$ s^{-1} (mean $\pm$ s.e.). The shapes of the graphs are typical of approximately half of the strands measured, although the position of the curve with respect to both axes varied. (*a*) Complex modulus as a function of strain. The graph of the elastic modulus looks very similar to this curve. (*b*) Tan δ as a function of strain. The graph of the viscous modulus looks very similar to this curve.

significantly higher in the presence of magnesium (Fig. 3, *a*, *b*, and *c* and Fig. 6, *a*, *b*, and *c*). Tan δ was unchanged (Figs. 3 *d* and 6 *d*). The work of Pollard and Mooseker (1981) showed that there is an increase in the equilibrium constant for monomer addition to purified rabbit skeletal muscle actin if $MgSO_4$ is present in the buffer solution, resulting in longer actin polymers. The presence in the cytoplasm of relatively longer actin filaments could lead to the increase in moduli reported here (Wainwright et al., 1976). The data also indicate that the presence of magnesium does not necessarily change the amount of energy stored relative to the amount dissipated (i.e., relative energy loss, tan δ, was unaffected).

[ATP]. Overall mean values of E*, E′, and E″ were significantly lower in the absence of ATP (Fig. 3, *a*, *b*, and *c*, and Fig. 7, *a*, *b*, and *c*). Again, tan δ was unaffected by this treatment (Figs. 3 *d* and 7 *d*). The decrease in cytoplasmic stiffness observed in preparations that lacked ATP was unexpected. Because in skeletal muscle ATP is involved in the release of actin–myosin cross-links, it has been thought that ATP would have the same function in nonmuscle cells. Thus, one might predict some form of cellular 'rigor', or increase in stiffness, upon removal of ATP because of the resulting cross-linking of the actomyosin network. The observations in this study suggest that there is no such rise in

stiffness associated with the removal of ATP from *Physarum* cytoplasm, although changes in stiffness that occurred in the 1–3 min between submersion in the medium and initiation of measurements would not have been recorded. Nonetheless, no lasting increase in stiffness was seen. A further result of the ATP removal experiments is interesting in that the viscous modulus was lower in the absence of ATP. These results all suggest that ATP may not function solely in the dissociation of actin–myosin in this system. Rather, these data are more consistent with a model in which the primary effect of [ATP] is on the polymerization of actin. ATP can raise the polymerization constant of actin (Pollard et al., 1982). Thus, in the absence of ATP, the actin network could begin to fall apart. Such a decrease in integrity of the cytoskeleton could lead to the observed decreases in complex and elastic moduli, while the decrease in length of actin filaments could lead to the observed decrease in viscous modulus (Wainwright et al., 1976). The magnesium data are also consistent with a polymerization hypothesis for the same reasons; both elastic and viscous moduli are higher in the presence of magnesium ions that raise the polymerization constant of actin.

Discussion

Summary

The purpose of this study was to refine our current understanding of the process of cell shape change by producing an extensive mechanical portrait of *Physarum* cytoplasm. Such a portrait describes the response of cytoplasm to mechanical loads such as those produced by actomyosin- or microtubule-based systems. This characterization is important for understanding processes such as cytokinesis, locomotion, and epithelial folding. During those processes the reaction of the cell to the forces generated by the cytoskeleton (or by other cells) is as fundamental to the functioning of the cell as the forces themselves. This work characterized the mechanical properties that determine those reactions, and explored their regulation by varying both chemical and mechanical conditions.

The results presented here indicate that E*, a measure of *Physarum* cytoplasm stiffness, and E′, a measure of its elasticity, are of the magnitude 10^4 N/m² under the mechanical and chemical conditions tested. For comparison, E′ of rubber is $\sim 7 \times 10^6$ N/m² at low strains and strain rates (Gordon, 1976). The data show a positive effect of $[Ca^{2+}]$ and $[Mg^{2+}]$ on stiffness that is because of an effect on both the elastic and the viscous moduli. Relative energy loss, tan δ does not change under any of the circumstances examined. This work also showed that stiffness decreases with an increase in strain or strain rate. The data indicate that removal of ATP lowers the viscous as well as the elastic component of stiffness. Finally, it was found that unlike skeletal muscle which undergoes a stiffening known as rigor when ATP is removed, stiffness of *Physarum* cytoplasm decreased in the absence of ATP.

Previous researchers have measured the longitudinal tension that was actively developed by a contracting strand (e.g., Nagai et al., 1978; Yoshimoto and Kamiya, 1978; Ueda et al., 1978; Götz van Olenhusen and Wohlfarth-Bottermann, 1979; Yoshimoto et al., 1981a,b). A sliding filament mecha-
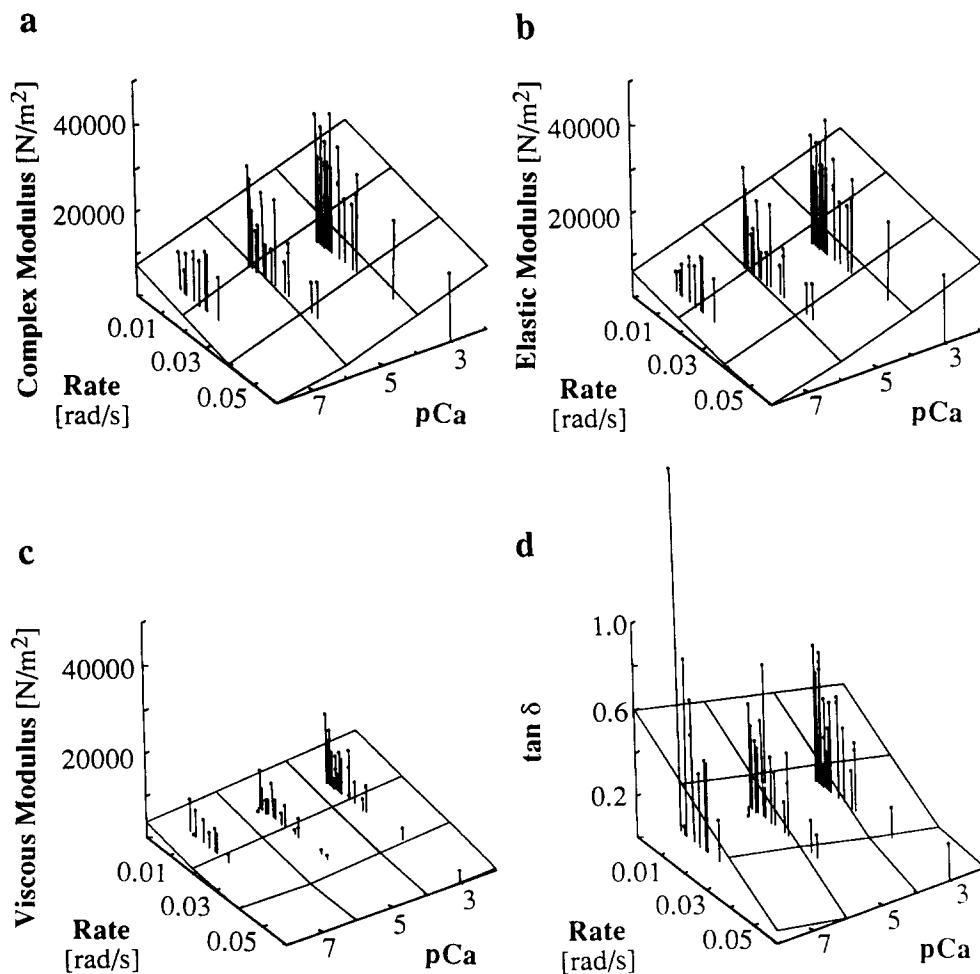
a

Complex Modulus [N/m^2]

40000

20000

0.01
0.03
0.05

Rate
[rad/s]

7   5   3

pCa

b

Elastic Modulus [N/m^2]

40000

20000

0.01
0.03
0.05

Rate
[rad/s]

7   5   3

pCa

c

Viscous Modulus [N/m^2]

40000

20000

0.01
0.03
0.05

Rate
[rad/s]

7   5   3

pCa

d

1.0

0.6

tan δ

0.2

0.01
0.03
0.05

Rate
[rad/s]

7   5   3

pCa

Figure 5. Mechanical properties of cytoplasm under conditions of varied strain rate and [Ca^{2+}] in the absence of Mg^{2+}. For clarity of presentation individual data points are connected by a line to the x–y plane and a plane representing a linear regression through the data has been added. Strain was held constant at 0.0026 ± 0.00021 (mean $\pm$ s.e.); $n = 47$ for all graphs. (a) The complex modulus, E*, increased with increasing calcium concentration ($p < 0.001$) and decreased with increasing strain rate ($p = 0.025$). (b) The elastic modulus, E', increased with increasing calcium concentration ($p < 0.001$) but was not correlated with strain rate ($p = 0.068$). (c) The viscous modulus, E", varied directly with calcium ($p = 0.012$) but was not correlated with strain rate ($p = 0.099$). (d) Tan δ, the relative energy loss, was not correlated with calcium ($p = 0.204$) or strain rate ($p = 0.108$).

nism has been proposed to explain this contraction, indicating the belief that this force generation is analogous to the tension developed in a skeletal muscle cell (Ogihara, 1982). The stiffness or resistance to deformation measured in the current experiments may, but does not necessarily, reflect this kind of tension generation by the strand. An increase in stiffness may reflect an increase in tension, but it may also simply reflect an increase in the number of tension resisting elements, e.g., cross-links or entanglements in the tension-resisting apparatus of the cell. The difference is important because the latter mechanism does not lead to a change in rest length.

Limitations of the Data

The interpretation of these results may be confounded by possible unknown effects of permeabilizing the *Physarum* plasma membrane with saponin. Two potential consequences of a leaky membrane are: (a) Loss of important cytoplasmic or membrane bound regulatory proteins, and (b) loss of structural integrity between the cytoplasm and the membrane. However, other workers have used permeabilized or membrane-free systems when studying force production by *Physarum* (Götz von Olenhusen and Wohlfarth-Bottermann, 1979; Yoshimoto et al., 1981a; Ogihara, 1982; Ogihara et al., 1983). Those studies show that cyclic force production continues in a strand with a compromised or absent mem-

brane, suggesting that at least one force-generating process and its machinery are unaffected by membrane removal.

The application of these data is also limited by the range of mechanical conditions tested. For example, it is known that externally imposed initial strains of 30–50% will greatly increase the tension generated by a *Physarum* strand during the contraction–relaxation cycle (Yoshimoto and Kamiya, 1978). Such large strains were specifically avoided in these experiments because of the extreme nonlinearity in mechanical behavior that would preclude linear analysis and use of the Fourier transform. There is, though, evidence that initially imposed strains as small as 10% can likewise lead to an increase in tension generated by a strand (Kamiya, 1981). It is not clear how imposed strains might affect passive cytoplasmic stiffness. However, an increase in tension produced by an actively contracting strand would be reflected as an increase in stiffness as measured in the current experiments. Thus, the magnitude of the values reported herein may be overestimates of unstrained cytoplasmic stiffness. In addition, the range of strains and strain rates that could be tested was limited by the experimental apparatus. Changes in mechanical properties due to strains or rates smaller than those tested could prescribe to the conditions and forces necessary to initiate deformation. Likewise, larger strains have been proposed to affect cell mechanical properties (Oster and Odell, 1984).
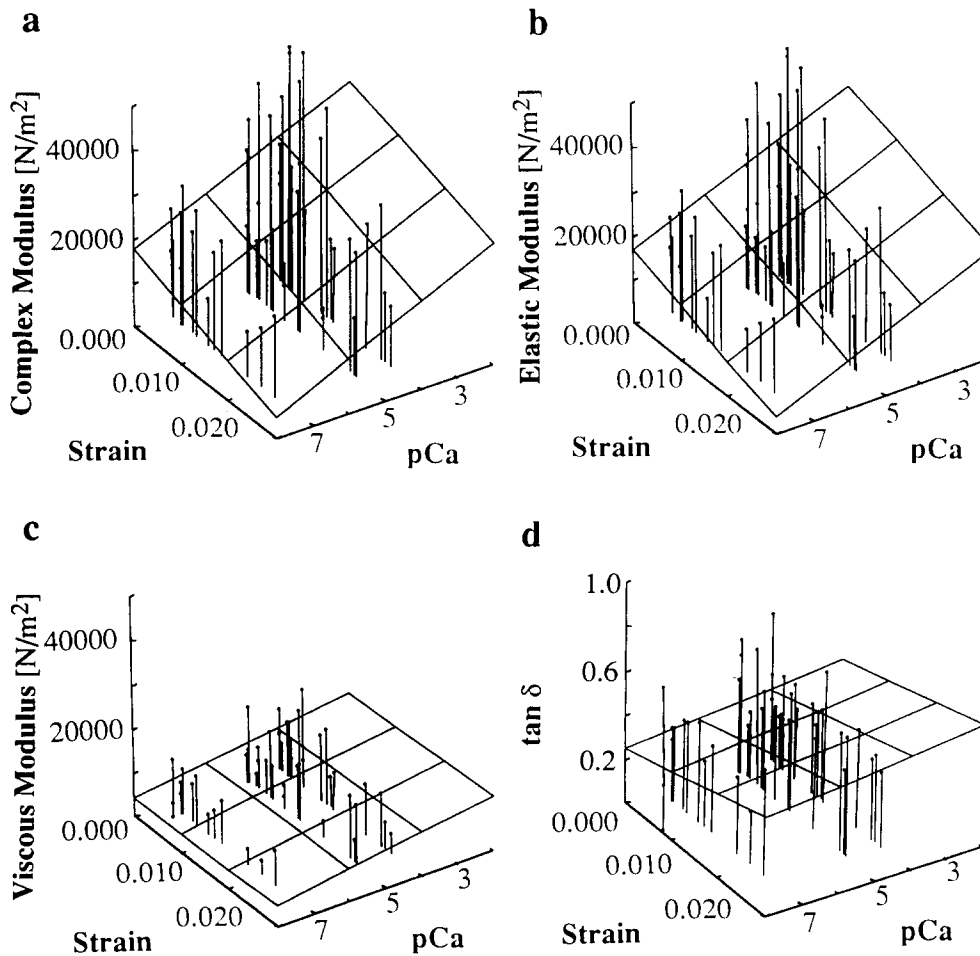
Figure 6. Mechanical properties of cytoplasm under conditions of varied strain and $[Ca^{2+}]$ in the presence of Mg^{2+}. For clarity of presentation individual data points are connected by a line to the x–y plane and a plane representing a linear regression through the data has been added. Strain rate was constant at 0.013 ± 0.00023 s^{-1} (mean $\pm$ s.e.); n = 56. (*a*) E*, the complex modulus, varies positively with calcium concentration (p < 0.001) and negatively with strain (p = 0.001); The overall mean value of E* was significantly greater in the presence of Mg^{2+} (Tukey HSD, χ^2 = 23.979, p = 0.003). (*b*) The elastic modulus, E', varied with both calcium concentration (p < 0.001) and strain (p = 0.001). The overall mean value of E' was significantly higher in the presence of Mg^{2+} (Tukey HSD, χ^2 = 23.246, p = 0.002). (*c*) E", the viscous modulus, varied directly with calcium concentration (p < 0.001) but was not correlated with strain in this data set (p = 0.751). The overall mean value of E" was significantly higher in the presence of Mg^{2+} (Tukey HSD, χ^2 = 29.389, p = 0.006). (*d*) The relative energy loss, tan δ, was independent of calcium concentration (p = 0.226). In this, and only this data set, tan δ showed dependence on strain (p = 0.014). Tan δ was unaffected by the presence of Mg^{2+} (Tukey HSD, χ^2 = 8.347, p = 0.989).

Effects of the Chemical Environment

The data are consistent with, and expand on, many previous studies of the mechanical properties of *Physarum* cytoplasm. For example, Ueda et al. (1978) and Ogihara (1982) found an increase in force generation with increasing $[Ca^{2+}]$. The present study indicates a positive correlation between $[Ca^{2+}]$ and stiffness. While the limit of resolution of the technique used here does not allow for an exact measurement of differences in stiffness between physiologically relevant $[Ca^{2+}]$'s (in *Physarum*, pCa ≈ 6–4) the overall trend suggests that such differences are present.

The interaction of actin and myosin in *Physarum* is ultimately regulated by $[Ca^{2+}]$ via its positive regulation of myosin light chain kinase (Ogihara et al., 1983). Thus an increase in $[Ca^{2+}]$ could lead to (*a*) an increase in the number of actin–myosin cross-links in the network or (*b*) active tension generation. Either phenomenon could result in an increase in elastic modulus. An increase in $[Ca^{2+}]$ might also raise the elastic modulus by releasing an actin filament binding protein or proteins thus permitting active sliding of the actin. This hypothesis is better explored in Condeelis (1983). $[Ca^{2+}]$ had no effect on tan δ, the relative energy loss (Figs. 3 *d*, 5 *d*, 6 *d*, and 7 *d*).

These results do not conspicuously reflect the influence of fragmin, a Ca^{2+}-activated actin severing protein present in *Physarum* cytoplasm (Hasegawa et al., 1980). Possible explanations include that this technique is insensitive to small scale differences in properties; that the influence of actin severing proteins contributes directly to the properties measured and therefore can not be measured as distinct from those properties; or that the influence of those enzymes is too local or rapid to be measurable using this kind of averaging technique. If this last explanation is valid, it may indicate that the action of those enzymes is not crucial to cell shape changes that, like this technique, take place over comparatively long times.

The positive effect of ATP observed in these experiments agrees with the work of Matsumura et al. (1980) who found that tension produced by a prepared *Physarum* actin–myosin thread increased as [ATP] was raised from 1 to 20 μM. However, these data disagree with the conclusion of Ogihara (1982) who found that a *Physarum* strand treated with the detergent Triton-X and suspended vertically in media of different ion and ATP concentrations elongates in the presence of 2.5 or 5.0 mM ATP (concentrations much higher than those used in the present experiments) but does not elongate if ATP is absent. He interprets elongation as indicating relaxation of the cytoplasm, and concludes that ATP functions in ac-
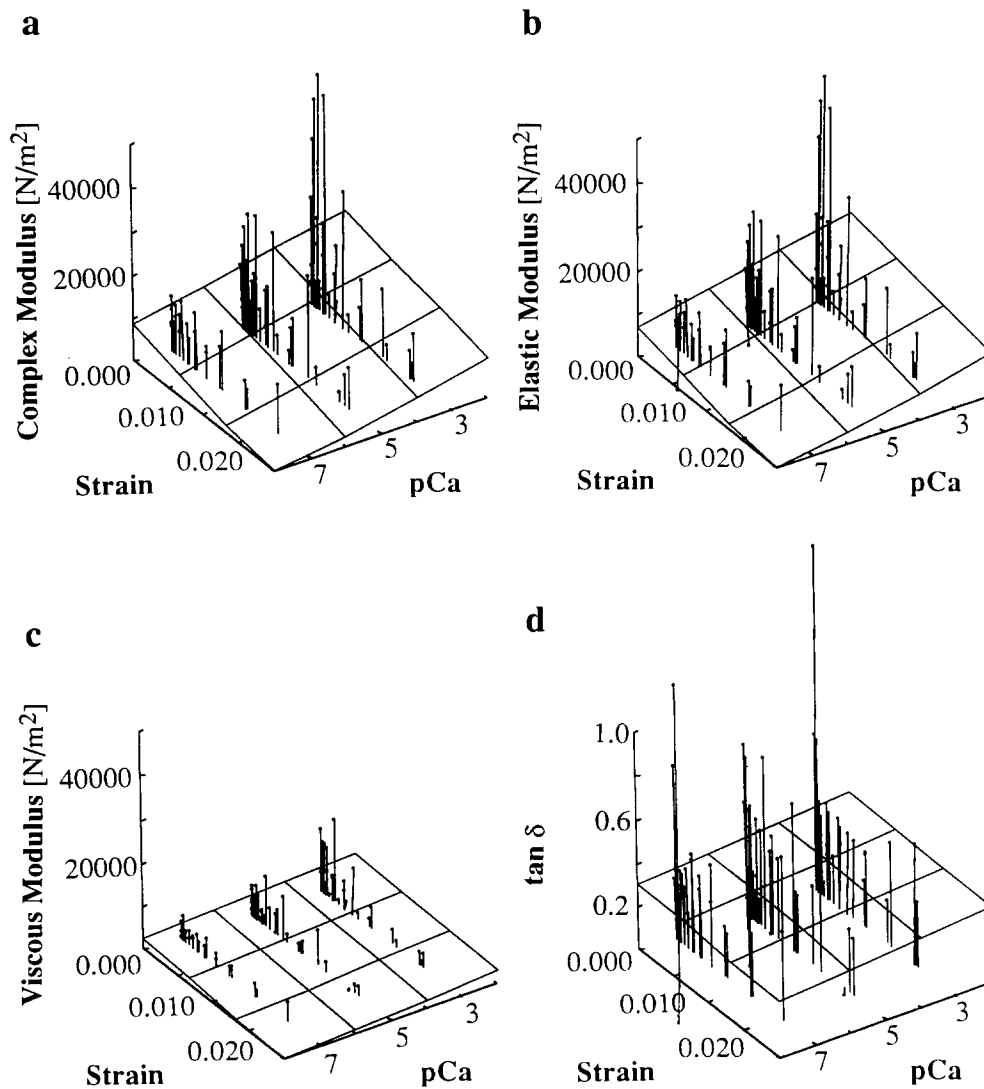
a

b

c

d

Figure 7. Mechanical properties of cytoplasm under conditions of varied strain and $[Ca^{2+}]$ in the absence of both ATP and Mg^{2+}. For clarity of presentation individual data points are connected by a line to the x-y plane and a plane representing a linear regression through the data has been added. Strain rate was constant at 0.018 ± 0.00063 s^{-1} (mean $\pm$ s.e.); n = 94. (*a*) E*, the complex modulus, varies positively with calcium concentration (p < 0.001) and negatively with strain (p = 0.015). The overall mean value of E* was significantly lower in the absence of ATP (Tukey HSD, χ^2 = 23.979, p = 0.001). (*b*) The elastic modulus, E', varied positively with calcium concentration (p < 0.001). In this, but only this data set, E' did not vary significantly with strain (p = 0.079). The overall mean value of E' was significantly lower in the absence of ATP (Tukey HSD, χ^2 = 23.246, p = 0.003). (*c*) E", the viscous modulus, varied directly with calcium concentration (p < 0.001). Although in this data set E" did not vary significantly with strain (p = 0.070), statistical conclusions from these data were sensitive to the effect of two strands. When the data from each of those strands was excluded from the analysis, the effect of strain became significant (p = 0.031, p = 0.047). Moreover, when the three data sets that examined strain effects were combined, the effect of strain on E" was highly significant (p = 0.002). The overall mean value of E" was significantly lower in the absence of ATP (Tukey HSD, χ^2 = 29.389, p = 0.006). (*d*) The relative energy loss, tan δ, was independent of calcium concentration (p = 0.402) and strain (p = 0.828). Tan δ was likewise unaffected by the absence of ATP (Tukey HSD, χ^2 = 8.347, p = 0.832).

tin–myosin dissociation. Further evidence in support of this hypothesis is that the strand elongates in the presence of an inorganic pyrophosphate that cannot be hydrolyzed but that does lead to actin–myosin dissociation.

Another interpretation of Ogihara's data is that ATP may simply be triggering the normal processes that lead to elongation/locomotion of the *Physarum* slime mold, but that those processes can be independent of ATP hydrolysis. Because the strands are not under tension (suspending strands in medium effectively removes the influence of gravity), this seems a possible explanation of the observed elongation. This interpretation is consistent with the hypothesis that ATP functions in actin polymerization (Pollard et al., 1982; see below).

Effects of the Mechanical Environment

In addition to the above experiments examining the effects of the chemical environment on *Physarum* cytoplasm, experiments have also been done that explore mechanical deter-

minants of cytoplasmic properties. In their study of *Physarum* endoplasm, Sato et al. (1983) conclude that endoplasm is non-newtonian. They also conclude that endoplasm is not a shear thinning material, i.e., viscosity does not decrease as strain rate increases. The data presented in this paper agree with that conclusion. However, the strain rate data set presented here is small (*n* = 10 strands, yielding 47 data points). When rate effects were examined in the larger strain data set, the viscous modulus was found to vary negatively with strain rate (data not shown), suggesting thixotropy. The discrepancy between this work and that of Sato et al., if it is real, could arise because the two sets of experiments cover different ranges of rates, or because Sato et al. looked exclusively at endoplasm while this study yielded measures integrated over the entire strand. Nevertheless, a true comparison is confounded by the use of different experimental techniques and conditions and by vastly different measurement scales.

These data also disagree with the results of researchers

studying purified actin preparations, for example Sato et al. (1987) and Zaner and Hartwig (1988). Those experiments indicate a positive correlation between strain rate and properties that are proportional to the complex modulus. Thus, the negative correlation reported here was unexpected. This correlation was, however, not strong, (p = 0.025) and in fact, the correlation between the strain rate and the elastic modulus (which is proportional to complex modulus) was not significant (p = 0.068); therefore, caution should be used in interpreting these data. However, even if the negative correlation seen in these data is not real, there is no evidence at all for a positive correlation like that reported by Sato et al. (1987) and by Zaner and Hartwig (1988). Perhaps the crucial difference between these experiments is the use of preparations of purified actin and actin-associated proteins as compared with preparations of whole cytoplasm. These two types of materials could have very different properties. In fact, Zaner and Hartwig (1988) show that even the process of gel filtration changes the properties of purified actin gels. These differences certainly suggest a general need for care when comparing in vitro and in vivo studies.

The other mechanical parameter that was varied in these experiments was the magnitude of the strain. In all cases, statistical analysis indicated that moduli vary inversely with strain. This result, like the strain rate result, confirms that the properties of cytoplasm are modulated by mechanical loading. The consequence of that modulation is that cytoplasm becomes easier to deform once deformation has begun. The data represented by Fig. 4, however, suggest that there may be a significant nonlinearity in the behavior of the material. Indeed, at the moment a cell begins to move the properties of the cytoplasm and the direction of change of those properties may be quite different from the properties of an already moving cell.

The relative loss of energy in the material, tan δ, remained constant under practically all of the experimental regimes. It is intriguing to consider the possibility that cytoplasmic properties can change significantly without incurring extra costs in terms of relative energy loss. However, caution in making such a conclusion is warranted. In one set of experiments (Fig. 6 d) tan δ did vary significantly with strain. Moreover, in more than half of the strands tested, the relationship of tan δ to strain looked like that shown in Fig. 4 b. Using a linear model to analyze the data loses whatever information is contained in the shape of that curve. If the pattern represented by the data shown in Fig. 4 b is the better representation of the general behavior of cytoplasm, then these data suggest that a series of small movements, during which cytoplasm would be relatively more viscous (tan δ higher), could lead to permanent shape change whereas cells could rebound from larger deformations because the cytoplasm would be relatively more elastic (tan δ lower). This idea that cells could exploit the changing properties of cytoplasm to accomplish either temporary or permanent shape changes was first proposed in Sato et al. (1987) with regard to different rates of deformation.

Implications of the Data

These data have implications for at least one widely accepted model of cytogel behavior. Specifically, the positive correlation between [Ca²⁺] and elastic modulus, E′, is not consis-

tent with the prediction of Oster and Odell's (1984) model of cytogel behavior. In that work, E′ is predicted to rise initially as [Ca²⁺] is raised, then fall at high [Ca²⁺]'s as the actin network is broken apart by calcium-activated actin-fragmenting proteins. This relationship is essential to the model's potential to simulate cell behavior leading to the bending of epithelial sheets (Oster and Odell, 1984). The model of epithelial folding presented in Odell et al. (1981) is also based on this mechanism. Those models also assume constant viscosity, a prediction that is also refuted by these data. Revising those models to reflect variable viscosity and the relationship between [Ca²⁺] and E′ observed in these experiments would likely lead to qualitatively different behavior by the model's solutions.

For a motile cell, an important consequence of the properties described herein is that stiffness decreases as strain or strain rate increases. In other words, motion becomes easier as the motion grows. The statistical analysis further indicates that a cell's resistance to deformation is highest when it is still. Thus, a still cell can exploit cytoplasmic stiffness to maintain its shape. If, however, the nonlinearity illustrated in Fig. 4 is real, a cell's resistance to deformation is lowest when it is subjected to strains approaching zero while being highest at strain rates approaching zero. The exact nature of the interplay between the opposite affects of small strain and low strain rate will have important implications for both the maintenance of cell shape and the initiation of cell shape change.

If the structural stability of the cytoplasm were determined exclusively by an extensively cross-linked network, one might predict that the viscous modulus of cytoplasm would be insignificant. These data, however, suggest that energy dissipation (i.e., viscosity) is an important component of the behavior of cytoplasm. Future models of cytoplasmic behavior should take into account both the magnitude of the viscous modulus and its dependence on [Ca²⁺] and, probably, strain.

References

Achenbach, U., and K. E. Wohlfarth-Bottermann. 1980. Oscillating contractions in protoplasmic strands of Physarum. J. Exp. Biol. 85:21–31.

Adams, D. S. 1990. Dynamic mechanical properties of Physarum cytoplasm. In Biomechanics of Active Movement and Deformation of Cells. N. Akkas, editor. Springer-Verlag, Berlin, Germany. 423–428.

Belintsev, B. N., L. V. Beloussov, and A. G. Zaraisky. 1987. Model of pattern formation in epithelial morphogenesis. J. Theor. Biol. 129:369–394.

Burnside, B. 1973. Microtubules and microfilaments in amphibian neurulation. Am. Zool. 13:989–1006.

Byers, B., and K. Porter. 1964. Oriented microtubules in elongating cells of the developing lens rudiment after induction. Proc. Natl. Acad. Sci. USA. 52:1091–1099.

Camp, W. G. 1936. A method of cultivating myxomycete plasmodia. Bull. Torrey Bot. Club. 63(4):205–210.

Condeelis, J. 1983. Rheological properties of cytoplasm: significance for the organization of spatial information and movement. Mod. Cell Biol. 2:225–240.

Elson, E. L. 1988. Cellular mechanics as an indicator of cytoskeletal structure and function. Ann. Rev. Biophys. Biophys. Chem. 17:397–430.

Fabiato, A., and F. Fabiato. 1979. Calculator programs for computing the composition of the solutions containing multiple metals and ligands used for experiments in skinned muscle cells. *J. Physiol. (Paris)*. 75:463–505.

Ferry, J. D. 1980. Viscoelastic Properties of Polymers. John Wiley & Sons, Inc., New York. 482 pp.

Gordon, J. E. 1976. The New Science of Strong Materials. Princeton University Press, Princeton, NJ. 287 pp.

Götz von Olenhusen, K., and K. E. Wohlfarth-Bottermann. 1979. Effects of caffein and D_2O on persistence and de novo generation of intrinsic oscillatory contraction automaticity in *Physarum*. *Cell Tissue Res.* 197:479–499.

Hasegawa, T., S. Takahashi, H. Hayashi, and S. Hatano. 1980. Fragmin: a calcium ion sensitive regulatory factor on the formation of actin filaments. *Biochemistry*. 19:2677–2683.

Hiramoto, Y. 1970. Rheological properties of sea urchin eggs. *Biorheology*. 6:201–234.

Hiramoto, Y. 1976. Mechanical properties of sea urchin eggs III. Viscoelasticity of the cell surface. *Dev. Growth & Differ.* 18:377–386.

Kamiya, N. 1959. Protoplasmic streaming. *Protoplasmatologia*. VIII,3a:1–199.

Kamiya, N. 1981. Physical and chemical basis of cytoplasmic streaming. *Ann. Rev. Plant Physiol.* 32:205–236.

Matsumura, F., Y. Yoshimoto, and N. Kamiya. 1980. Tension generation by actomyosin thread from a non-muscle system. *Nature (Lond.)*. 285:169–171.

Meyhöfer, E., and T. Daniel. 1990. Dynamic mechanical properties of extensor muscle cells of the shrimp *Pandalus danae*: cell design for escape locomotion. *J. Exp. Biol.* 151:435–452.

Miller, R. J. 1988. Calcium signaling in neurons. *Trends Neurosci.* 11:415–419.

Mittenthal, J., and R. M. Mazo. 1983. A model for shape generation by strain and cell-cell adhesion in the epithelium of an arthropod leg segment. *J. Theor. Biol.* 100:443–483.

Murakami, A. 1987. Control of ciliary beat frequency in the gill of *Mytilus*. II: effects of saponin and BRIJ-58 on the lateral cilia. *Comp. Biochem. Physiol.* 86:281–287.

Nagai, R., Y. Yoshimoto, and N. Kamiya. 1978. Cyclic production of tension force in the plasmodial strand of *Physarum polycephalum* and its relation to microfilament morphology. *J. Cell Sci.* 33:205–225.

Odell, G. M., G. Oster, P. Alberch, and B. Burnside. 1981. The mechanical basis of morphogenesis. I. Epithelial folding and invagination. *Dev. Biol.* 85:446–462.

Ogihara, S. 1982. Calcium and ATP regulation of the oscillatory torsional movement in a triton model of *Physarum* plasmodial strands. *Exp. Cell Res.* 138:377–384.

Ogihara, S., and Y. Tonomura. 1982. A novel 36,000-dalton actin binding protein purified from microfilaments in *Physarum* plasmodia which aggregates actin filaments and blocks actin-myosin interaction. *J. Cell Biol.* 93:604–614.

Oster, G. F., and G. M. Odell. 1984. The mechanochemistry of cytogels. *Physica* 12D:333–350.

Oster, G. F., J. D. Murray, and A. K. Harris. 1983. Mechanical aspects of mesenchymal morphogenesis. *J. Embryol. Exp. Morph.* 78:83–125.

Pollard, T. D., and S. Ito. 1970. Cytoplasmic filaments of Amoeba proteus I. The role of filaments in consistency changes and movement. *J. Cell Biol.* 46:267–289.

Pollard, T. D., and M. S. Mooseker. 1981. Direct measurement of actin polymerization rate constants by electron microscopy of actin filaments nucleated by isolated microvillus cores. *J. Cell Biol.* 88:654–659.

Pollard, T. D., U. Aebi, J. A. Cooper, W. E. Fowler, and P. Tseng. 1982. Actin structure, polymerization, and gelation. *In* Organization of the Cytoplasm. Cold Spring Harbor Symposia on Quantitative Biology. Cold Spring Harbor Laboratory, Cold Spring Harbor, NY. XLVI:513–524.

Priess, J. R., and D. I. Hirsh. 1986. *Caenorhabditis elegans* morphogenesis: the role of the cytoskeleton in elongation of the embryo. *Dev. Biol.* 117:156–173.

Rappaport, R. 1967. Cell division: direct measurement of maximum tension exerted by furrow of echinoderm eggs. *Science (Wash. DC)*. 156:1241–1243.

Sato, M., T. Z. Wong, and R. D. Allen. 1983. Rheological properties of living cytoplasm: endoplasm of *Physarum plasmodium*. *J. Cell Biol.* 97:1089–1097.

Sato, M., W. H. Schwartz, and T. D. Pollard. 1987. Dependence of the mechanical properties of actin/α-actinin gels on deformation rate. *Nature (Lond.)* 325:828–830.

Seifriz, W. 1952. Rheology in cells. *In* Deformation and Flow in Biological Systems. A. Frey-Wyssling, editor. North Holland Publishing Company, Amsterdam. 3–156.

Spooner, B. S., and N. K. Wessells. 1972. An analysis of salivary gland morphogenesis: role of cytoplasmic microfilaments and microtubules. *Dev. Biol.* 27:38–54.

Stopak, D., and A. K. Harris. 1982. Connective tissue morphogenesis by fibroblast traction. I. Tissue culture observations. *Dev. Biol.* 90:383–398.

Stout, M. A., and F. P. J. Diecke. 1983. Ca distribution and transport in saponin skinned vascular smooth muscle. *J. Pharmacol Exp. Ther.* 225:102–111.

Taylor, D. L., J. S. Condeelis, P. L. Moore, and R. D. Allen. 1973. The contractile basis of amoeboid movement. I. The chemical control of motility in isolated cytoplasm. *J. Cell Biol.* 59:378–394.

Tidball, J. G., and T. L. Daniel. 1986. Elastic energy storage in rigored skeletal muscle cells under physiological loading conditions. *Am. J. Physiol.* 250:56–64.

Ueda, T., K. Götz von Olenhusen, and K. E. Wohlfarth-Bottermann. 1978. Reaction of the contractile apparatus in *Physarum* to injected Ca^{++}, ATP, ADP and 5'AMP. *Cytobiologie: Eur. J. Cell Biol.* 18:76–94.

Waddington, C. H. 1942. Observations on the forces of morphogenesis in the amphibian embryo. *J. Exp. Biol.* 19:284–293.

Wainwright, S. A., W. D. Biggs, J. D. Currey, and J. M. Gosline. 1976. Mechanical Design in Organisms. Princeton University Press, Princeton, NJ. 423 pp.

White, J. G., and G. G. Borisy. 1983. On the mechanisms of cytokinesis in animal cells. *J. Theor. Biol.* 101:289–316.

Wohlfarth-Bottermann, K.-E. 1987. Dynamic organization and force production in cytoplasmic strands. *In* Cytomechanics. J. Bereiter-Hahn, O. R. Anderson, and W.-E. Reif, editors. Springer-Verlag, Berlin, Germany. 154–166.

Yoshimoto, Y., and N. Kamiya. 1978. Studies on contraction rhythm of the plasmodial strand II. Effect of externally applied forces. *Protoplasma*. 95:101–109.

Yoshimoto, Y., F. Matsumura, and N. Kamiya. 1981a. Simultaneous oscillations of Ca^{2+} efflux and tension generation in the permeabilized plasmodial strand of *Physarum*. *Cell Motil.* 1:433–443.

Yoshimoto, Y., T. Sakai, and N. Kamiya. 1981b. ATP oscillation in *Physarum* plasmodium. *Protoplasma*. 109:159–168.

Zaner, K. S., and J. H. Hartwig. 1988. The effect of filament shortening on the mechanical properties of gel-filtered actin. *J. Biol. Chem.* 263(10):4532–4536.

Zar, J. H. 1984. Biostatistical Analysis. 2nd ed. Prentice-Hall Inc., Englewood Cliffs, NJ. 718 pp.